

## Extrinsic magnetoresistance in magnetite nanoparticles

Kai Liu,<sup>a)</sup> L. Zhao, and P. Klavins

*Department of Physics, University of California, Davis, California 95616*

Frank E. Osterloh and H. Hiramatsu

*Department of Chemistry, University of California, Davis, California 95616*

(Presented on 14 November 2002)

Magnetite ( $\text{Fe}_3\text{O}_4$ ) nanoparticles, 8 to 9 nm in size, have been synthesized using an aqueous precipitation technique. X-ray diffraction and chemical titration confirm a single cubic spinel phase with expected stoichiometry. Superparamagnetic behavior has been observed in pressed pellets of the nanoparticles above 200 K. Spin-dependent tunneling through adjacent particles has led to a negative magnetoresistance,  $-8.6\%$  at 200 K and  $-4.5\%$  at 300 K in a 70 kOe field. This is caused by the field-induced alignment of the nanoparticle magnetization directions. © 2003 American Institute of Physics. [DOI: 10.1063/1.1556133]

Significant magnetoresistance (MR) effects have been reported in compact powder pellets of high spin-polarization materials, such as  $\text{CrO}_2$  and  $\text{Fe}_3\text{O}_4$ .<sup>1-3</sup> The size of the powders studied has ranged from a few hundred nanometers to tens of microns. It is desirable to investigate such spin-dependent transport phenomenon in assemblies of even smaller nanoparticles. Fundamentally, new physics may emerge as the physical dimensions become comparable to certain characteristic length scales, such as single-domain particle size and spin-flip diffusion length.<sup>4,5</sup> Practically, arrays of nanoparticles with small size distributions and shape variations may lead to ultrasmall magnetic devices.<sup>6,7</sup> In this work, we report the investigation of magnetism and MR in 8 to 9 nm magnetite ( $\text{Fe}_3\text{O}_4$ ) nanoparticle pellets. We have observed a spin-dependent tunneling through contiguous nanoparticles that is caused by the relative alignment of the particle magnetizations.

Nanoparticles of  $\text{Fe}_3\text{O}_4$  have been synthesized by an aqueous precipitation technique, by mixing ferric and ferrous chloride (with a 2:1 molar ratio) with aqueous ammonia.<sup>8-10</sup> After synthesis, the nanoparticles were collected by magnetic decantation, washed with water, and dried *in vacuo*. No surfactants were used in the synthesis in order to minimize the contact resistance between particles. According to infrared spectroscopy (compacted sample in KBr), the neutralized nanoparticles are coated with adsorbed water molecules [ $\nu(\text{O}-\text{H}) = 3420 \text{ cm}^{-1}$ ]. An x-ray diffraction pattern ( $\text{Cu K}\alpha$ ) of the synthesized black  $\text{Fe}_3\text{O}_4$  nanoparticles is shown in Fig. 1, along with the Joint Committee on Powder Diffraction Standards (JCPDS) reference patterns of magnetite and a structurally similar maghemite ( $\gamma\text{-Fe}_2\text{O}_3$ ).<sup>10</sup> A clean  $\text{Fe}_3\text{O}_4$  cubic inverse spinel phase is confirmed. A key distinction is the  $\text{Fe}_3\text{O}_4$  (222) peak at around  $37^\circ$ . In comparison, although the main  $\gamma\text{-Fe}_2\text{O}_3$  peaks are similar to the  $\text{Fe}_3\text{O}_4$  ones, the noticeable absence of all other peaks whose intensities are comparable to the one at  $37^\circ$  is a telltale sign of the absence of  $\gamma\text{-Fe}_2\text{O}_3$ . Using an internal Si reference to

calibrate any peak position shift due to the diffraction sample preparation, we have determined the cubic lattice parameter of  $\text{Fe}_3\text{O}_4$  to be 0.8384 nm. Additionally, the diffraction peaks are broadened due to the nanometer size of the crystallites. From the full width at half maximum of the peaks, corrected for instrumentation width, we have derived an average grain size of about 9 nm. This is in agreement with transmission electron microscopy and atomic force microscopy studies which show an average size of  $8 \pm 2 \text{ nm}$ .<sup>9</sup> We have also used a ferrous sulfate and potassium permanganate titration method<sup>11</sup> to independently verify the stoichiometry of the  $\text{Fe}_3\text{O}_4$  nanoparticles. The ratio of  $\text{Fe}^{3+}:\text{Fe}^{2+}$  agrees with the expected 2:1 ratio within 7%.

For this study, we have prepared compact pellets of  $\text{Fe}_3\text{O}_4$  by cold-pressing bare  $\text{Fe}_3\text{O}_4$  nanoparticles into a 6 mm die under a  $2 \times 10^7 \text{ Pa}$  pressure for 10 min. This leads to compact pellets with 40% packing density.<sup>12</sup> Magnetic measurements have been performed by a superconducting quantum interference device (SQUID) magnetometer. Electrical leads are attached by silver paint onto pressed pellets to al-

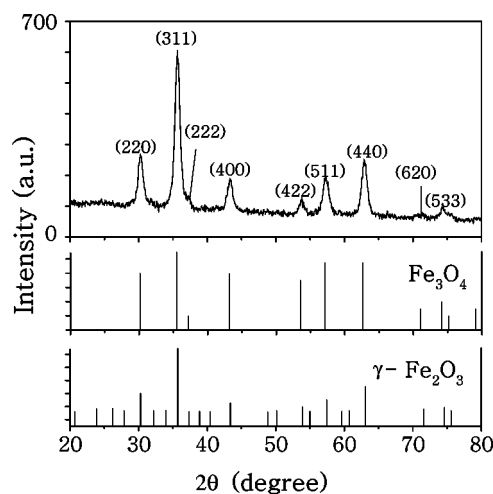


FIG. 1. Powder x-ray diffraction pattern of  $\text{Fe}_3\text{O}_4$  nanoparticles, along with JCPDS reference patterns of magnetite and maghemite ( $\gamma\text{-Fe}_2\text{O}_3$ , No. 25-1402), all shown in linear scale.

<sup>a)</sup>Electronic mail: kailiu@ucdavis.edu

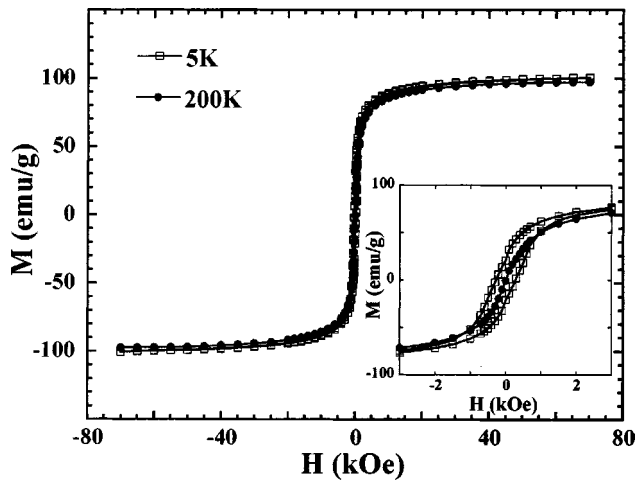


FIG. 2. Magnetic hysteresis loops of the magnetite pellet at 5 K (open square) and 200 K (closed circle). The inset shows a magnified view near zero field.

low four-point transport measurements. Due to the large resistance of the pellet, several  $M\Omega$  at 300 K, a Keithley 617 electrometer with a 200  $G\Omega$  impedance has been used for the transport measurements.

Magnetic hysteresis loops of a pellet are shown in Fig. 2. At 5 K, a ferromagnet-like hysteresis loop is seen, with a coercivity of 290 Oe. At high fields, 20–70 kOe, the magnetization displays a linear slope beyond saturation, due to the ferrimagnet nature of  $Fe_3O_4$ . Extrapolating the linear slope towards zero field leads to a saturation magnetization  $M_S$  of about 95 emu/g, consistent with the bulk value of 98 emu/g at 0 K.<sup>13</sup> At increasing temperatures, the saturation magnetization decreases slightly whereas the coercivity diminishes precipitously. At 200 K, the hysteresis has collapsed (Fig. 2 inset) and the sample becomes superparamagnetic. The blocking behavior is due to the small size of the particle where thermal fluctuations dominate. It is also confirmed by measuring the temperature dependence of the magnetization during zero-field cooling and field-cooling, as well as by measuring the temperature dependence of the remanent magnetization after saturation at 5 K. Note that the 200 K blocking temperature measured is technique-specific, determined by the sampling time. In our case, the measurement time is about 30 s for any temperature point.

The temperature dependence of resistivity is shown in Fig. 3(a), in zero field and a 70 kOe field. At 300 K and zero field, the resistivity  $\rho$  is  $8 \times 10^3 \Omega m$ , about seven orders of magnitude larger than the  $\sim 2 \times 10^{-4} \Omega m$  resistivity seen in bulk single crystals and thin films,<sup>2,14</sup> and four orders of magnitude larger than the  $\sim 10^{-1} \Omega m$  seen in pressed pellet of 50  $\mu m$  sized magnetite powders (also 40% packing density).<sup>2</sup> With decreasing temperatures,  $\rho$  increases almost exponentially from  $8 \times 10^3 \Omega m$  at 300 K to  $1 \times 10^8 \Omega m$  at 110 K, below which the resistance values were beyond our instrument capabilities. The activation energy deduced from  $\rho - T$  over 200–300 K is about 280 meV, much larger than the 20–40 meV previously seen in  $Fe_3O_4$  thin films.<sup>15</sup> The much larger  $\rho$  and activation energy indicate that most of the resistance comes from the contacts between nanoparticles.

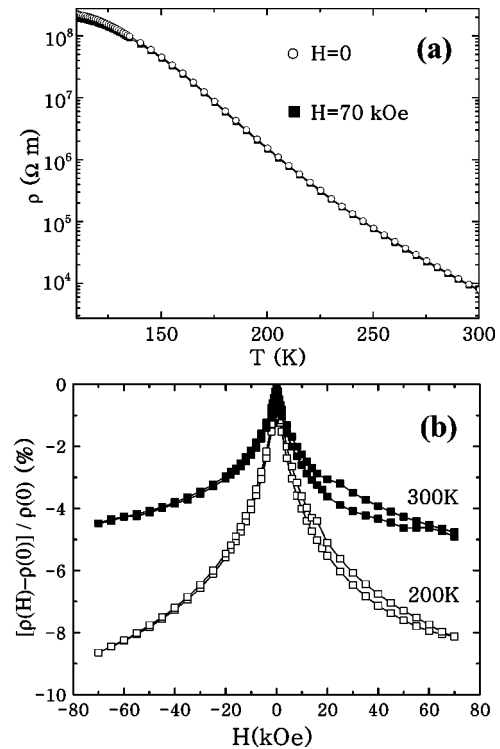


FIG. 3. (a) Temperature dependence of resistivity in zero field (open circle) and a 70 kOe field (closed square) from 300 to 110 K. (b) Field dependence of magnetoresistance of a  $Fe_3O_4$  nanoparticle pellet at 200 and 300 K.

This could also mask the appearance of a Verwey transition.<sup>16</sup> An average per contact resistance can be estimated by  $\rho/d = 8 \times 10^{11} \Omega$ , where  $d$  is the particle size. Similar to earlier studies,<sup>2,3</sup> this contact resistance value is much larger than the quantum limit of a metallic contact:  $h/2e^2 = 13 k\Omega$ . Thus the electron transport is limited by interparticle tunneling.<sup>17</sup> In a 70 kOe field, the resistivity is slightly lower, while following qualitatively the same temperature dependence as in zero field.

The field-dependence of MR, defined as  $[\rho(H) - \rho(0)]/\rho(0)$ , has been measured at 200 and 300 K, as shown in Fig. 3(b). Negative MR of  $-8.6\%$  and  $-4.5\%$  have been observed in a field of 70 kOe at 200 and 300 K, respectively. It is remarkable that despite the much larger resistance in the present nanoparticle pellet, the MR effect is comparable to those obtained in much less resistive samples.<sup>2,3</sup> For example, at 300 K and 12 kOe, we observed a MR effect of 2.5%, slightly larger than the 1.7% and 1.2% observed previously in polycrystalline and pressed powder (50  $\mu m$  size) samples.<sup>3</sup> Furthermore, the MR is nonhysteretic at both temperatures, except a small drift within the error of the experiment. This correlates with the collapse of coercivity in the magnetic hysteresis loop of the pellet at 200 K and above, caused by the superparamagnetism. In comparison, in previous polycrystalline and pressed powder pellets with much larger grain sizes, the coercivity is finite and the MR displays a double-peak feature at the coercive fields.<sup>3</sup>

The negative MR is due to the spin-dependent tunneling through a network of contiguous nanoparticles. In zero magnetic field, the magnetization  $M$  of each nanoparticle orients largely in random, which represents a spin-disordered state.

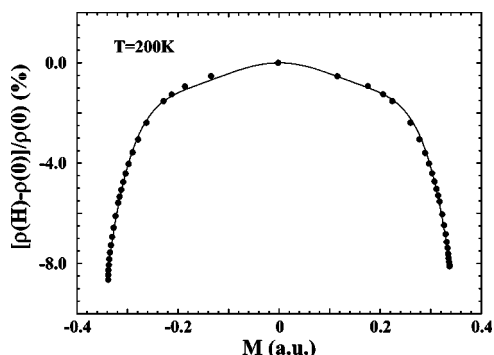


FIG. 4. Correlation between magnetoresistance MR and magnetization  $M$  at 200 K. The solid line is a fit to high order terms of  $M^2$ .

The application of a magnetic field aligns all magnetizations and reduces the spin disorder. This in turn increases the spin-dependent tunneling probability and leads to a reduction in resistance, hence the negative MR. This is analogous to the giant magnetoresistance (GMR) effect seen in metallic granular solids with magnetic granules embedded in a non-magnetic matrix.<sup>18</sup> There, the GMR is due to a spin-dependent scattering mechanism. In the present case, the extrinsic MR can also be correlated to a factor  $\langle \cos \phi_{ij} \rangle$ , where  $\phi_{ij}$  is the angle between magnetization directions of two nanoparticles. In the case of independent nanoparticles,  $\text{MR} \sim \langle \cos \phi_{ij} \rangle \sim \langle \cos \theta \rangle^2 \sim (M/M_s)^2$ , where  $\theta$  is the angle between the magnetization direction of a nanoparticle and the applied field.<sup>18</sup> Since saturation magnetization  $M_s$  is a constant, MR can be compared with  $M^2$ . In our nanoparticle pellet, however, we observe clear deviations from a quadratic dependence between MR and  $M$ , particularly at low  $M$  values. The departures can be corrected by adding higher order terms of  $M^4$  and  $M^6$ . A fit to  $\text{MR} = aM^2 + bM^4 + cM^6$  is shown in Fig. 4, where  $a$ ,  $b$ , and  $c$  are fitting parameters. This is due to the strong coupling between the  $\text{Fe}_3\text{O}_4$  nanoparticles that cause deviations from the independent particle scenario.

In summary, we have investigated magnetic and transport properties of pressed  $\text{Fe}_3\text{O}_4$  nanoparticle pellets. The assembly becomes superparamagnetic above 200 K over a 30 s time scale. Spin-dependent tunneling through contiguous nanoparticles depends on the relative alignment of their magnetizations, resulting in an extrinsic and significant negative MR.

This work has been supported by University of California-Davis Faculty Research Grant and start-up funds.

- <sup>1</sup>J. M. D. Coey, A. E. Berkowitz, L. Balcells, F. F. Putris, and A. Barry, *Phys. Rev. Lett.* **80**, 3815 (1998).
- <sup>2</sup>J. M. D. Coey, A. E. Berkowitz, L. Balcells, F. F. Putris, and F. T. Parker, *Appl. Phys. Lett.* **72**, 734 (1998).
- <sup>3</sup>J. M. D. Coey, *J. Appl. Phys.* **85**, 5576 (1999).
- <sup>4</sup>For a recent review, see for example, J. I. Martin, J. Nogués, K. Liu, J. L. Vicent, and I. K. Schuller, *J. Magn. Magn. Mater.* **256**, 449 (2003).
- <sup>5</sup>See for example, K. Liu, K. Nagodawithana, P. C. Searson, and C. L. Chien, *Phys. Rev. B* **51**, 7381 (1995).
- <sup>6</sup>C. T. Black, C. B. Murray, R. L. Sandstrom, and S. Sun, *Science* **290**, 1131 (2000).
- <sup>7</sup>K. Liu, J. Nogués, C. Leighton, H. Masuda, K. Nishio, I. V. Roshchin, and I. K. Schuller, *Appl. Phys. Lett.* **81**, 4434 (2002).
- <sup>8</sup>R. Massart, *IEEE Trans. Magn.* **MAG-17**, 1247 (1981).
- <sup>9</sup>T. Fried, G. Shemer, and G. Markovich, *Adv. Mater.* **13**, 1158 (2001).
- <sup>10</sup>Other known phases of  $\gamma\text{-Fe}_2\text{O}_3$  similarly have a large number of small peaks that do not coincide with the cubic magnetite peak positions.
- <sup>11</sup>K. Liu, X. W. Wu, K. H. Ahn, T. Sulchek, C. L. Chien, and J. Q. Xiao, *Phys. Rev. B* **54**, 3007 (1996).
- <sup>12</sup>The packing density is the ratio of the pellet density over that of the  $\text{Fe}_3\text{O}_4$  x-ray density.
- <sup>13</sup>J. Smit and H. P. J. Wijn, *Ferrites* (Wiley, New York, 1959).
- <sup>14</sup>G. Q. Gong, A. Gupta, G. Xiao, W. Qian, and V. P. Dravid, *Phys. Rev. B* **56**, 5096 (1997).
- <sup>15</sup>B. Raquet, J. M. D. Coey, S. Wirth, and S. Von Molnár, *Phys. Rev. B* **59**, 12435 (1999).
- <sup>16</sup>A Verwey transition in similarly prepared magnetite nanoparticles was observed at a lower temperature of 96 K, see P. Poddar, T. Fried, and G. Markovich, *Phys. Rev. B* **65**, 172405 (2002).
- <sup>17</sup>We expect the contact resistance to decrease with increasing particle size and packing density as the corresponding number of conduction paths is reduced.
- <sup>18</sup>J. Q. Xiao, J. S. Jiang, and C. L. Chien, *Phys. Rev. Lett.* **68**, 3749 (1992).